Electrochimica Acta xxx (2016) xxx-xxx

Contents lists available at ScienceDirect

Electrochimica Acta

journal homepage: www.elsevier.com

Review Article

Graphitic Carbon Nitride as a Catalyst Support in Fuel Cells and Electrolyzers

Noramalina Mansor [a, 1], Thomas S. Miller [b, 1], Ishanka Dedigama [a], Ana Belen Jorge [c], Jingjing Jia [d], Veronika Brázdová [b], Cecilia Mattevi [d], Chris Gibbs [e], David Hodgson [f], Paul R. Shearing [a], Christopher A. Howard [g], Furio Corà [b], Milo Shaffer [d], Daniel J.L. Brett [a, *], Paul F. McMillan [b, *]

[a] Electrochemical Innovation Lab, Department of Chemical Engineering, University College London, London WC1E 7JE, United Kingdom
[b] Department of Chemistry, University College London, 20 Gordon Street, London WC1H 0AJ, United Kingdom
[c] Materials Research Institute, School of Engineering and Materials Science, Queen Mary University of London, London E1 4NS, United Kingdom
[d] Department of Chemistry, Imperial College London, London SW7 2AZ, United Kingdom
[e] UCL Business Plc, The Network Building 97 Tottenham Court Road, London W1T 4TP, United Kingdom
[f] Amalyst Ltd, Faraday Wharf, Innovation Birmingham Campus, Birmingham Science Park Aston, Birmingham B7 4BB, United Kingdom
[g] Department of Physics & Astronomy, University College London, London, WC1E 6BT, United Kingdom

ARTICLE INFO

Article history:
Received 13 July 2016
Received in revised form 31 October 2016
Accepted 2 November 2016
Available online xxx

Keywords:
electrocatalyst support materials
oxygen reduction
hydrogen oxidation
electrolysis
N-doped carbon
graphitic carbon nitride

ABSTRACT

Electrochemical power sources such as polymer electrolyte membrane fuel cells (PEMFCs) require the use of precious metal catalysts, which are deposited as nanoparticles onto supports in order to minimize their mass loading and therefore cost. State-of-the-art/commercial supports are based on forms of carbon black. However, carbon supports present disadvantages including corrosion in the operating fuel cell environment and loss of catalyst activity. Here we review recent work examining the potential of different varieties of graphitic carbon nitride (gCN) as catalyst supports, highlighting their likely benefits, as well as the challenges associated with their implementation. The performance of gCN and hybrid gCN-carbon materials as PEMFC electrodes is discussed, as well as their potential for use in alkaline systems and water electrolyzers. We illustrate the discussion with examples taken from our own recent studies.

1. Introduction

The increasing demand for, but reducing supply of, traditional fossil fuels has driven efforts to develop cheap, abundant and environmentally friendly technologies for energy production, conversion and storage [1]. This has, in turn, led to dramatic improvements in the performance of hydrogen or methanol fuel cells and also in hydrogen-producing water electrolyzers. Despite these advances, current 'state-of-the-art' systems are still largely dependent on metals with low abundancies in the earth's crust, such as Pt, to provide the active catalyst components which can amount to as much as 42% of the total system cost [2,3]. A long-term goal is to reduce the use of these scarce metal catalysts, while simultaneously improving the lifetime and efficiency of the energy conversion devices. Most operating fuel cells incorporate a polymer electrolyte membrane (PEM) and operate in acidic electrolyte media. Using an alkaline electrolyte is one option for achieving cost reduction, as the oxygen reduction reaction (ORR) occurs more readily in alkaline media, it permits the use of non-precious metal cathode catalysts such as Ni, or lower Pt loading [4]. However, a commercial alkaline anion exchange membrane with comparable performance and durability to Nafion® (the leading acid based PEM material), has not yet been developed. Currently, intense research efforts are being directed at (i) lowering the Pt loading in PEM fuel cell (PEMFC) electrodes and improving their efficiency and durability, and (ii) seeking alternative catalyst systems. It has been shown that carbon nitride materials can play a key role in both of these target areas.

The catalysts used in fuel cells and electrolyzers are typically in the form of high surface area nanoparticles (NPs) with a narrow size distribution, which are deposited and dispersed uniformly on a high surface area support (~200–1000 $m^2 g^{-1}$), usually commercially available carbon black. The effect NP size and shape has on catalytic activity has been well documented in the literature, with studies reporting an ideal particle size of ~3 nm for maximum activity. This particle size has been shown to provide an optimal adsorption energy between the catalyst and reactants [5–7]. Making supported NP catalyst structures maximizes the electrochemically active surface area (ECSA) of the NPs while the amount of metal used is minimized, for greater efficiency at lower cost. Incorporation of a proton-conducting ionomer into this catalyst layer facilitates the formation of three-

* Corresponding authors.
Email addresses: d.brett@ucl.ac.uk (D.J.L. Brett); p.f.mcmillan@ucl.ac.uk (P.F. McMillan)

[1] NM and TSM have contributed equally to this work.

http://dx.doi.org/10.1016/j.electacta.2016.11.008
0013-4686/

phase boundary regions, where electrochemical reactions occur in contact between the catalyst, fuel and electrolyte [8].

Although most research has focused on development of the electrocatalysts (ECs), the nature of the support material and its interaction with the NPs are also crucial for effective electrode operation. The catalyst support determines the porosity, tortuosity and wettability of the electrode. It also influences the size distribution and stability of the deposited NPs, the ability to produce and infiltrate inks for deposition in membrane electrode assemblies (MEA), and the capacity to control the efficiency of electronic and chemical catalyst-support interactions [9–11]. An ideal catalyst support should (i) allow an even distribution of NPs across its surface for maximum ESCA to volume ratio; (ii) have a high electronic conductivity to contribute to the electrochemical functioning of the electrode; (iii) have a porous network structure over multiple length scales that enhances reactant access; (iv) exhibit high stability under both the operating and transient conditions of the specific application, which can periodically lead to potential excursions as high as 1.5 V, causing severe carbon corrosion on the electrode; (v) require minimal processing *via* chemical or thermal activation; (vi) be compatible with a range of catalyst fabrication processes and (vii) be manufactured by a low-cost process that is environmentally benign. These are a stringent set of conditions which must be met simultaneously.

Carbon black is used as the catalyst support material of choice in PEMFCs due to its ready availability, low cost, minimal environmental impact and favorable physical properties. However, carbon is well known to undergo electrochemical oxidation under fuel cell operating conditions and loss of catalytic activity during repeated cycling is known to occur [12,13]. This is because at the cathode the cell voltage typically changes from 0.55 to 0.90 V during transient operating conditions [14] and a PEMFC system goes through an estimated 38,500 start-stop cycles over its lifetime [14]. Additionally, during the shutdown and start-up steps, a H_2/air front is created at the anode, which drives the potential at the cathode above 1 V. Conversely, during operation, fuel starvation may occur in a localized area of the anode, leading to an increase in anode potential until water electrolysis occurs in order to sustain the cell current [15]. Loss of catalyst activity can take place through several mechanisms, including particle aggregation (Ostwald ripening), crystal migration, dissolution/precipitation, and carbon corrosion [16,17]. The catalyst/support interaction plays a major role in determining the extent of these processes. For example, Pt is known to act as a catalyst for carbon corrosion [18–21]; this means that Pt particles are more likely to become detached or 'orphaned' from the support because corrosion is enhanced at the interface between the two. The support is also responsible for determining the agglomerate structure and microstructure of the catalyst layer. An effective microstructure will create a well-connected, highly active ECSA and ensure efficient mass transport of reactants to the triple phase boundary (TPB) where the electrolyte, catalyst and fuel meet at a reactive site. Degradation of the support not only leads to a reduction in the ECSA, but also to a lowering of the rate of mass-transport, by blocking pores and modifying the surface roughness. Because of these issues there has been a drive to find a next generation of catalyst supports that exhibit high stability to corrosion and that interact beneficially with the catalyst particles. Alternative support materials should also offer the potential for improved intrinsic catalyst stability, but few materials simultaneously meet these requirements. For example, certain metal alloys that possess high catalytic activity, exhibit poor stability on conventional carbon supports. However, these metal-alloy catalysts may be feasible on an alternative support which 'anchors' the NPs more effectively, or that results in an electronically stabilizing effect.

A wide range of alternative catalyst supports have been tested, including advanced carbon materials such as carbon nanotubes, aerogels and graphene [22,23], non-carbon supports including tantalum oxyphosphate, titania, tin or indium oxides, tungsten carbide [24,25], as well as carbon doped with boron [26–29], sulphur [30,31], or phosphorous [32–34]. However, N-doped carbon supports are by far the most widely researched, particularly as spatial correlations have been shown to exist between regions of high N content and stabilized NPs [35,36]. N-doping is usually carried out post-synthesis, *via* treatment with NH_3 at elevated temperatures, resulting in N-doped carbons containing a few atomic percent N, randomly located throughout the material [35]. This approach provides little or no control over the nitrogen functionalities being introduced, which can be problematic as certain functionalities contribute in specific ways to the enhancement of catalytic effects [37]. For example, pyridinic N is suggested to form charge-transfer complexes with Pt [37], enhancing the kinetics of the ORR and methanol oxidation reaction (MOR), and preventing metal agglomeration during NP formation [36]. However the mechanistic details of these processes are yet to be fully understood. Furthermore, a strong NP attachment to the catalyst support is of little use if the surrounding, purely carbonaceous, matrix still suffers from corrosion [13]. To this end, there has been a move towards the development of more stable supports, including graphitic carbon nitrides (gCNs) that, in contrast with N-doped carbons, usually consist of a backbone of C—N bonds and contain a high concentration of N sites, located at defined positions within the layers [38–40]. Here we present a summary of recent results and future perspectives for using gCNs as catalyst support materials for fuel cells and water electrolyzers.

2. Graphitic carbon nitrides: material types and structures

Graphitic carbon nitride is a generic term applied to a large family of materials with different chemical and structural characteristics. In recent publications these have been increasingly referred to as "g-C_3N_4" compounds, but that is a misnomer: almost none of the materials concerned occur with a 3:4C:N ratio, they generally contain substantial concentrations of H and other elements (especially O), the "graphitic" layers are likely to be far from complete, and the sheet-like domains are unlikely to be planar [41,42]. Several separate classes of gCN materials have been identified. The first concerns graphitic carbon, graphene-like carbons or carbon nanotubes prepared with a degree of N incorporation which extends up to a few atomic per cent [43,44] and possess metallic properties [44,45]. They are most usefully termed N-doped carbons rather than gCNs. The use of this type of material as EC supports began in the 1980s [46,47], where carbonaceous materials pyrolyzed together with nitrogen-containing precursors were utilized. Since then, various other synthesis approaches have been shown to provide support materials that were found to improve the performance of the transition metal catalyst-support combinations [35,36,48–50].

The largest class of true carbon nitride compounds include a range of "graphitic" or polymeric structures with compositions extending along, or near, a tie-line between C_2N_3H and C_3N_4 in a ternary C—N—H phase diagram [42]. They are formed by condensation reactions from readily available precursors such as dicyandiamide, melamine or urea following thermal treatments in the 500–700 °C range [51]. These are most accurately termed gCNH compounds and their structures are usually based on linked heptazine (tri-*s*-triazine, C_6N_7) units. At lower synthetic temperatures, these polyheptazines (PHs) form poorly organized ribbon-like structures, such as those found in Liebig's melon [52], which are terminated laterally by -NH- and -NH_2

groups (Fig. 1a). As the processing temperature is raised, the degree of condensation increases with loss of NH_3 components, and sheet-like units begin to form "graphitic" structures. Theoretically, this process can be extended to the g-C_3N_4 composition (Fig. 1b), but this has not been observed in practice [41,51]. Instead, the limiting stoichiometries recorded so far among gCNH materials have been close to the C_2N_3H composition. A further class of carbon nitride structures is based on independent triazine (C_3N_3) rings linked together by -N= or -NH- groups. These polytriazine imide (PTI) layers provide an alternative solution to forming infinite graphitic sheets with the C_3N_4 composition (Fig. 1c,d). The first of these was prepared in nanocrystalline form using chemical vapor deposition (CVD) techniques [53,54]. Later, a crystalline triazine-based graphitic carbon nitride (TGCN, Fig. 1c) was discovered during a molten salt synthesis, deposited on the walls of the reaction vessel or at the surface of the melt phase [55]. In this material the layers are reported to contain C_6N_6 voids that are stacked according to an AB or ABC pattern [55]. The bandgap of this material was estimated to be 2.7 eV, although this does not explain the dark color of the synthesized material. The PTI family of crystalline gCN materials is extended by inclusion of heteroatoms such as H, Li, Br and Cl within the structure, which are introduced during the synthesis in a molten salt (e.g., LiCl:KBr) or by high pressure-high temperature routes [56–60]. These materials contain larger ($C_{12}N_{12}$) ring voids within the layers, with Cl^- or Br^- ions residing in the interlayer spaces or occupying the void sites. The triazine units are linked by -NH- groups that decorate the interior of the void sites, and the hydrogens can be fully or partially replaced by Li^+ cations. Additional Li^+ species can occur between the layers [58,59] (Fig. 1d, e).

3. gCN, gCNH and PTI materials as PEM fuel cell catalyst supports

gCNH and PTI materials are reported to be semiconductors with bandgaps in the 2.5–2.8 eV range [57]. That property leads to visible light absorption and their yellow to brown coloration. gCN compounds alone, or materials decorated with Pt, RuO_2 or related metal/metal oxide NPs as co-catalysts, have been reported to act as photocatalysts capable of splitting water into H_2 and O_2, as well as driving other redox reactions under simulated solar irradiation [61–63]. In their pure and doped form they have also been shown to exhibit redox catalytic behavior [64] and they have been tested for energy storage applications and as Li^+ battery anodes [65,66]. As these highly nitrided materials also have excellent mechanical, chemical and thermal resistance [61,63] they have the ability to survive even the harshest PEM fuel cell operating conditions. In addition, their structures typically contain a high concentration of N—H functional groups, as well as lone pairs present on the N atoms of the triazine or heptazine units, providing Brønsted acid and Lewis base sites and an abundance of tethering sites for the metal NPs. Combined, their intrinsic catalytic activity, their high stability, their unique termination chemistry and high surface area [63], has led to gCNH and PTI materials being developed as components in EC systems.

Insights into the improved chemical resistance of gCNH and PTI materials to corrosion, compared to carbon, can be obtained from simple band structure considerations (Fig. 2). The allowed energy states in conductive carbons span across the H^+/H_2 and O_2/H_2O potentials, and thus provide competitive redox sites accessible under

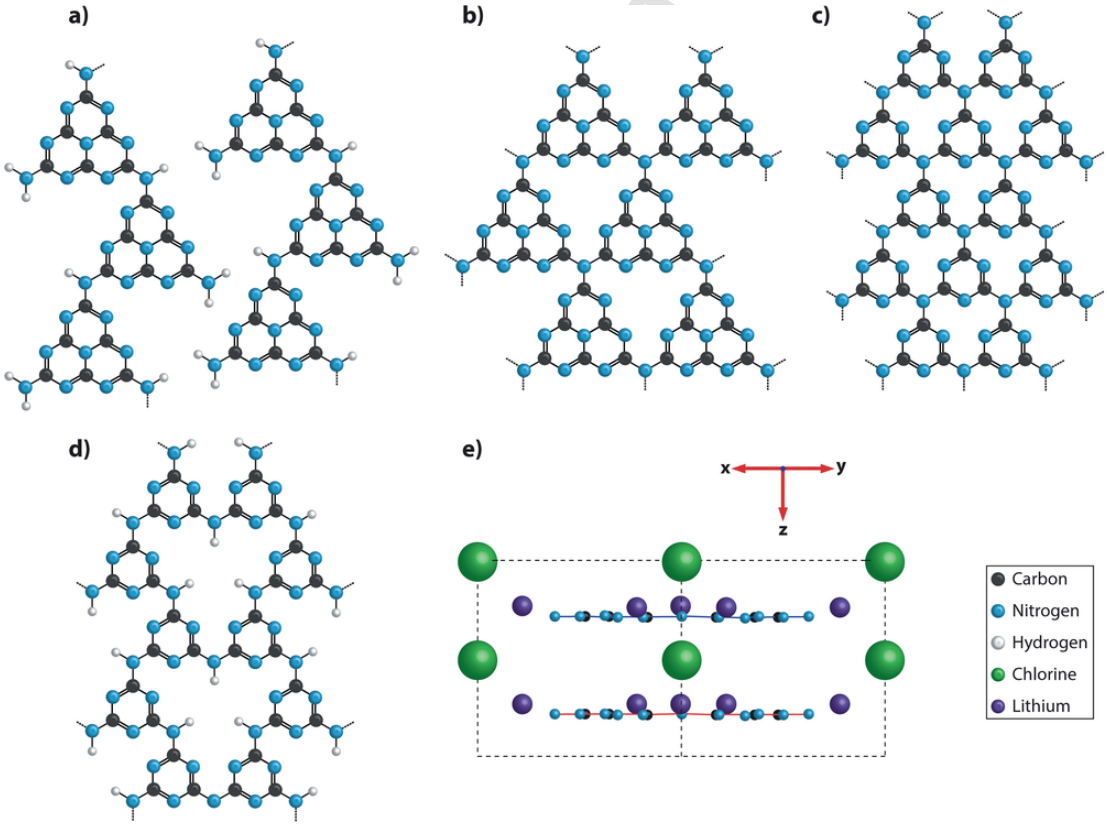

Fig. 1. Structural motifs found in graphitic carbon nitrides. (a) Liebig's melon ($[C_6N_7(NH_2)(NH)]_n$) contains zig-zag chains of heptazine (tri-s-triazine) units linked by bridging nitrogens and decorated on their edges by N-H groups, (b) fully condensed C_3N_4 layer based on heptazine units, (c) fully condensed C_3N_4 layer based on triazine units, (d) PTI backbone based on triazine ring units, linked by N-H bridges and e) Side elevation of fully occupied PTI.LiCl.

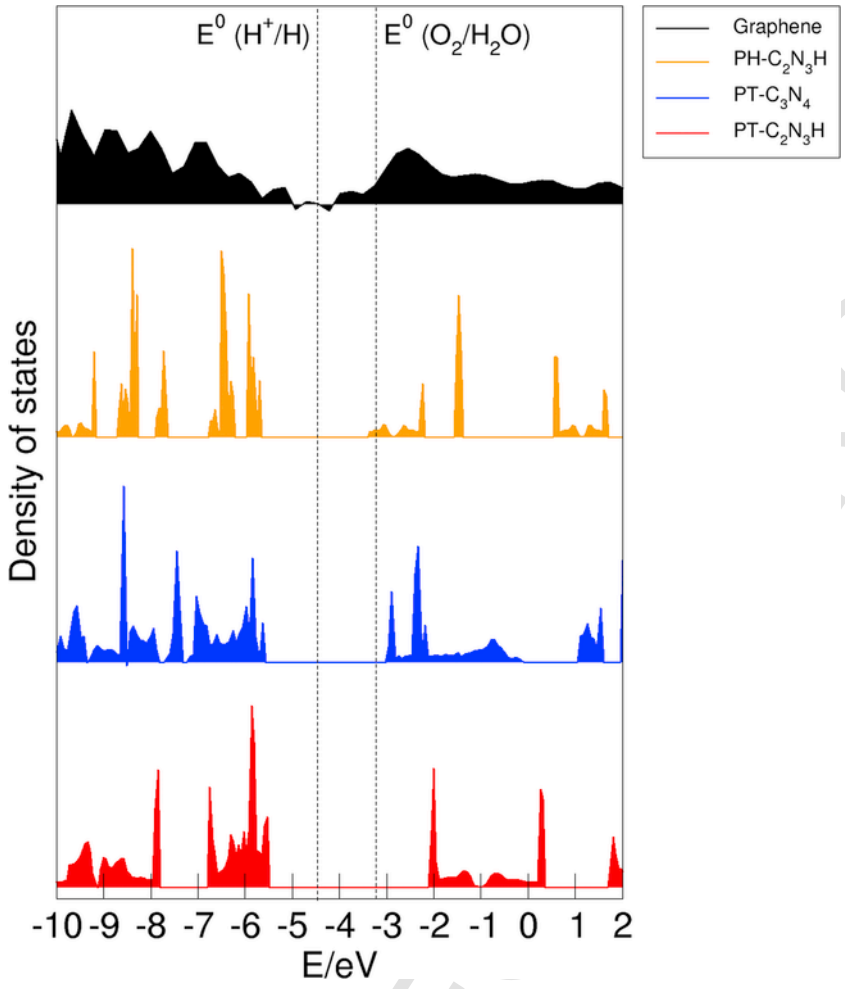

Fig. 2. Calculated electronic density of states for conductive C (graphene) and a selection of three representative layered gCN or gCNH structures including polyheptazine (PH) and polytriazine (PT) varieties of C_2N_3H, and one PT layer of g-C_3N_4. The calculations were carried out using density functional theory and the PBE functional under periodic boundary conditions. Vertical lines indicate the standard H^+/H_2 and O_2/H_2O potentials.

both hydrolysis and fuel cell conditions. In contrast, the C atoms in gCN, gCNH and PTI compounds are bonded to N atoms with fully satisfied valence states and are thus fully oxidized. This chemistry opens a band gap that brackets the H^+/H_2 and O_2/H_2O potentials and thus corrosion of the C—N backbone is thermodynamically unfavorable under electrochemical operation. It should, however, be remembered that most fuel cell electrode processes occur at potentials that do not match the theoretical thermodynamic values and that activation overpotentials play a significant role in the real-world fuel cell processes.

An early study of a gCNH material relevant to its behavior as a fuel cell EC, was carried out by Lyth et al., who investigated its intrinsic catalytic activity for the ORR [67]. Using material synthesized from cyanuric chloride, they demonstrated that the electrochemical ORR was efficiently catalyzed on gCNH when compared to carbon black. Unfortunately, the current density achieved was too low for use in practical applications. This was attributed to the low surface area and wide band gap of the material, which limited the activity of the electrode-reactant-electrolyte TPB. Upon blending with high surface area carbon, the performance improved as a result of the increased surface area and electronic conductivity. Aside from this intrinsic catalytic activity and enhanced durability, the abundant pyridinic sites within gCNH have been shown to provide anchoring sites for metal NPs, reducing aggregation and potentially enhancing the catalytic activity. Kim et al. showed that in a direct methanol fuel cell (DMFC), PtRu supported on gCNH exhibited 78–83% higher power density than the same catalyst deposited on carbon black [40]. In another study, Mansor et al. investigated gCNH and PTI materials as supports for chemically deposited Pt NPs [38]. Both materials displayed greater electrochemical stability than carbon black during accelerated corrosion testing. In particular, Pt supported on the highly crystalline PTI.LiCl showed excellent durability, as defined by changes in the ECSA under potential cycling, and this catalyst-support combination was found to have superior intrinsic methanol oxidation activity [38]. It is not yet known if the Li and Cl incorporated within the PTI materials played an active role in the EC, similar to that played by boron, which acts as a Lewis acid in B-doped carbon nitrides by reducing the electron density on C atoms [68]. It is possible their role was entirely passive and the increased crystallinity of the PTI was purely responsible for the observed improvement in durability.

A major obstacle to the use of metal-free gCNs as EC catalysts or as catalyst supports for metal NPs, is their poor conductivity. As discussed above, these gCN materials are semiconductors with band gaps up to 2.8 eV [57], which severely limits their intrinsic electrical conductivity and can negatively impact their practical application.

For example, Miller et al. showed that in gCNH based lithium-ion battery anodes, increased resistivity negatively impacted Li storage capacities [65]. However, when these materials are employed as an anodic catalyst support it has been found that the fast reaction kinetics of the hydrogen evolution reaction (HOR) compensate for the limitations of reduced conductivity (*vide infra*). On the other hand, the cathodic ORR is a slow process and ECs supported purely on gCN materials exhibit poor ORR performance. It is only when the gCNs are closely contacted with conductive materials (e.g. graphene) that efficient oxygen reduction is observed. As shown in the study by Kim et al. [40], gCN materials can be combined in a composite or hybrid electrode system along with conductive forms of carbon.

4. gCN/C composite/hybrid electrocatalysts and catalyst supports

4.1. Mixed gCN/C hybrid electrocatalysts and catalyst supports

First-principles theoretical studies using pure melem units ($C_6N_{10}H_6$) as a model for the behavior of gCNH, have shown that these materials have poor electron-transfer efficiency for the ORR, preferring the 2-electron over the direct 4-electron pathway and therefore producing an accumulation of poisoning intermediates, such as H_2O_2 [69]. The addition of a conductive substrate increases the number of electrons accumulated on the melem surface, and hence participating in the reaction, thereby facilitating the 4-electron ORR process (Fig. 3). Thusly, several studies have focused on testing the performance of gCN-carbon composite materials as metal-free catalysts and catalyst supports for fuel cell electrodes [70,71].

Graphene and the related material reduced graphene oxide (rGO) are popular choices of conducting substrate for gCNHs, due to their high surface area and electrical conductivity [72–74]. Furthermore, density functional theory (DFT) calculations for a PH model of a g-C_3N_4 material reveal strong electronic coupling and charge transfer at the interface with graphene, resulting in enhanced electronic conductivity of the gCN [75]. Early experimental reports on metal-free gCNH-graphene composite ECs show excellent ORR performance, especially in alkaline electrolytes [70,76,77]. It was also documented that metals such as Pd and PtRu supported on gCNH/rGO exhibited very high electrocatalytic activity for formic acid, methanol and ethanol oxidation reactions, as well as enhanced durability and alcohol tolerance [78,79]. These studies highlighted the importance of optimizing the gCN to graphene ratio in the composites to maintain the catalytic activity while improving the conductivity.

In our own recent work we have been examinining the performance of carbon nitride-rGO composites as an EC support for the ORR and HOR [80]. Here hybrid gCNH-rGO materials were synthesized from melamine and dicyandiamide dissolved in a GO solution, which was pyrolyzed under N_2 following water removal by freeze-drying (Fig. 4). From relative peak intensities in the X-ray photoelectron spectrum (Fig. 4a) we determined that the composite only contained ~30% graphene (rGO), with the remainder gCNH. Examination by scanning electron microscopy (SEM. Fig. 4b) showed a well-integrated composite structure, with rGO layers closely associated with gCNH to provide the necessary conductive backbone. Pt was subsequently deposited *via* a modified $NaBH_4$ assisted ethylene glycol reduction method, resulting in an excellent dispersion of Pt NPs on the support, with average particle size ~2.8 nm (Fig. 4d), as shown by transmission electron microscopy (TEM) images (Fig. 4c). The ECSA of Pt supported on the gCNH/rGO remained lower than commercial Pt/C, but it was three times higher than Pt on gCNH alone (Fig. 4e), indicating that the incorporation of rGO improves the electronic conductivity of the support and allowed electrical contact to a greater number of NPs.

Fig. 5 shows the ORR polarization curves, specific activity (SA) and mass activity (MA) of the material described above, other gCN

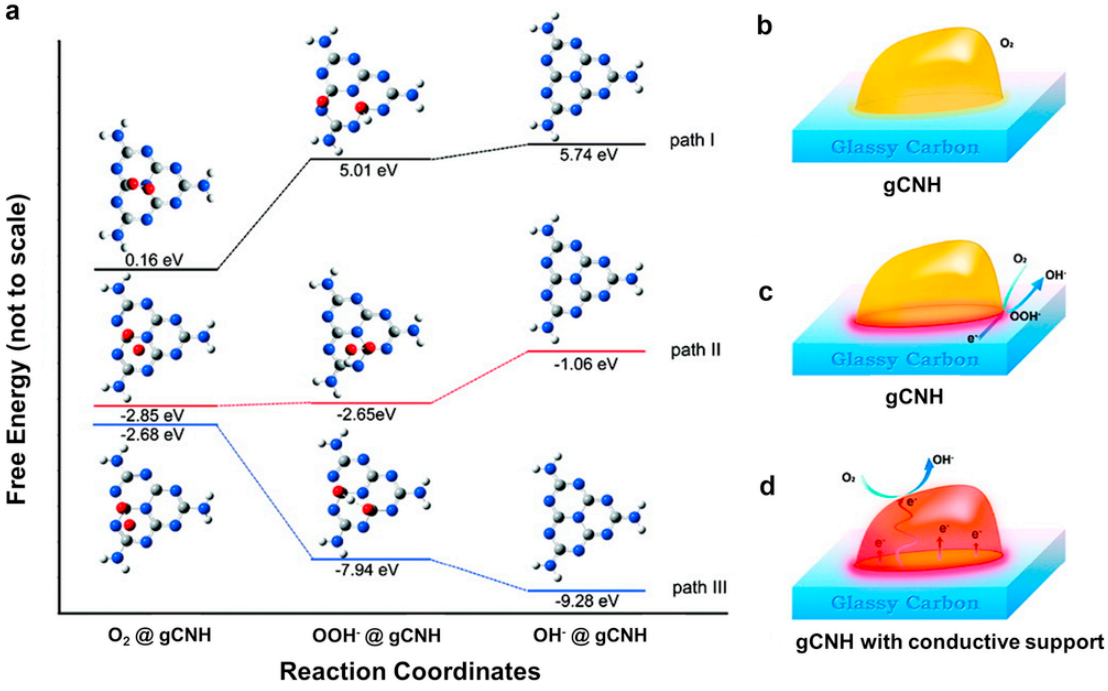

Fig. 3. (a) Free energy plots of ORR and geometry optimized configurations of adsorbed species on a model gCNH surface with zero (path I), two (path II), and four electron (path III) participations. Grey, blue, red and white represent C, N, O, H atoms, respectively. (b–d) Schematic pathway of ORR on gCNH with zero electron, gCNH with two electron participation, and gCNH – conductive support composite with four electron participation, respectively. Red areas represent the catalytically active sites. Reprinted and modified with permission from [69]. Copyright 2011 American Chemical Society.

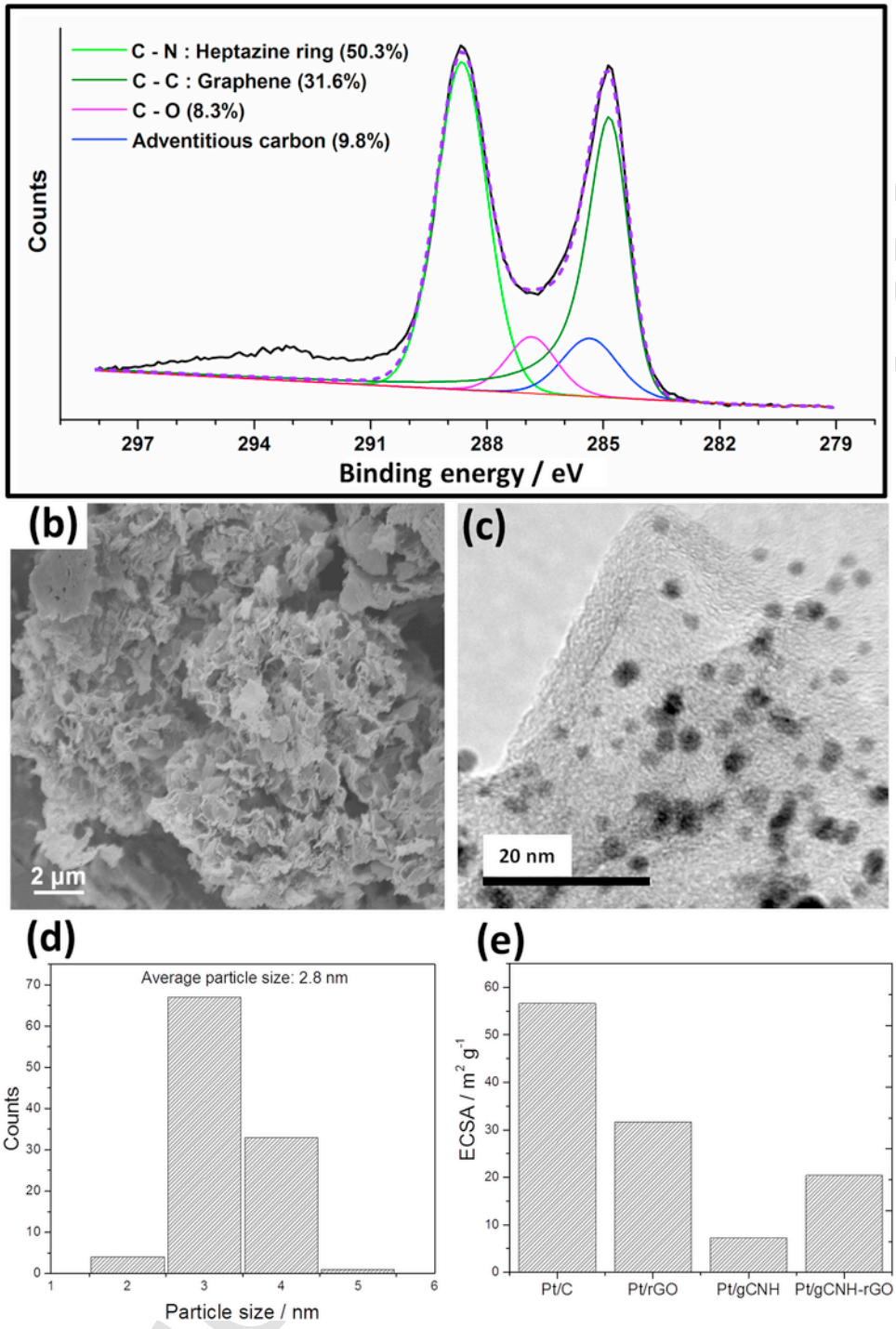

Fig. 4. gCNH-rGO composite structures (a) XPS spectrum of the C1s region of a gCNH-rGO composite prepared *via* simultaneous rGO reduction and gCNH formation reactions. (b) SEM image of gCNH-rGO composite synthesized by simultaneous rGO reduction and gCNH formation. (c) TEM image of Pt dispersion on gCNH-rGO composite. (d) Average particle size and size distribution of Pt nanoparticles. (e) ECSA of Pt on supports obtained from cyclic voltammetry in deoxygenated 0.1 M $HClO_4$.

supports and a commercial Pt/C at 0.90 V. These data were obtained from *ex situ* rotating disk electrode tests, where the SA and MA values for commercial Pt/C were comparable to those reported in the literature [81]. It was found that Pt on the gCNH-rGO composite had improved ORR activity over Pt/gCNH or Pt/rGO, despite the higher ECSA of the latter (Fig. 4e). The gCN containing materials also demonstrated SA at 0.90 V comparable to that of commercial Pt/C (~500 µA cm^{-2}). Although the overall MA was lower than commercial Pt/C, due to the lowered ECSA, these systems have considerable scope for optimization.

Although the incorporation of rGO into the composite resulted in an improvement in the electronic conductivity, the layered morphology of the graphene component limited the number of active sites and mass transport access for reactants, negatively affecting the ORR performance. The HOR performance of Pt/gCNH-rGO measured *in situ*

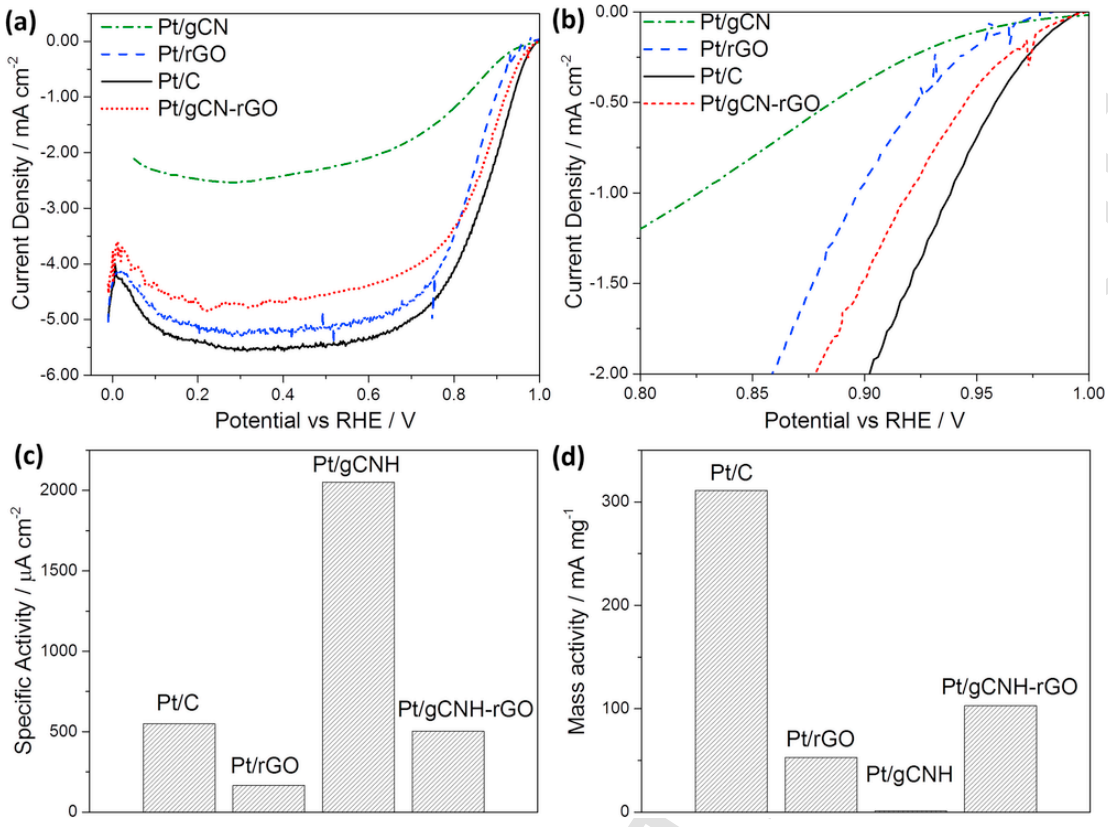

Fig. 5. (a) The ORR polarization curves of Pt/gCNH, Pt/rGO, Pt/C (Alfa Aesar), and Pt/gCNH-rGO at 1600 rpm in 0.1 M $HClO_4$. (b) Detail of the ORR polarization curves highlighting the overpotential region. (c) Specific activity and (d) Mass activity of the materials obtained at 0.90 V.

was, however, comparable to commercial Pt/C, as demonstrated in the fuel cell polarization curve in Fig. 6a. As the HOR is a very fast reaction [82], the lowered ECSA has less impact on the catalytic performance here.

As discussed above, fuel cell anodes often suffer from durability issues that result from normal fuel cell operation, which over time, corrode the electrode. However, long-term potential cycling durability tests show that our Pt/gCNH-rGO had improved stability over commercial Pt/C, as shown in Fig. 6b. This work therefore shows that gCNH-rGO hybrid materials are attractive as alternative, durable, anode catalyst support for PEM fuel cells. Further investigations are ongoing to further test the performance parameters, including electrode durability, in a real fuel cell configuration.

4.2. Three-dimensional (3D) gCN/C hybrid electrocatalysts and catalyst supports

Several routes for the fabrication of ordered 3D architectures of gCNH with a robust porous structure, high surface area, abundant N active sites and good electrical conductivity have been investigated. For example, 3D gCNH materials have been produced by thermal polycondensation of precursors deposited on a framework structure

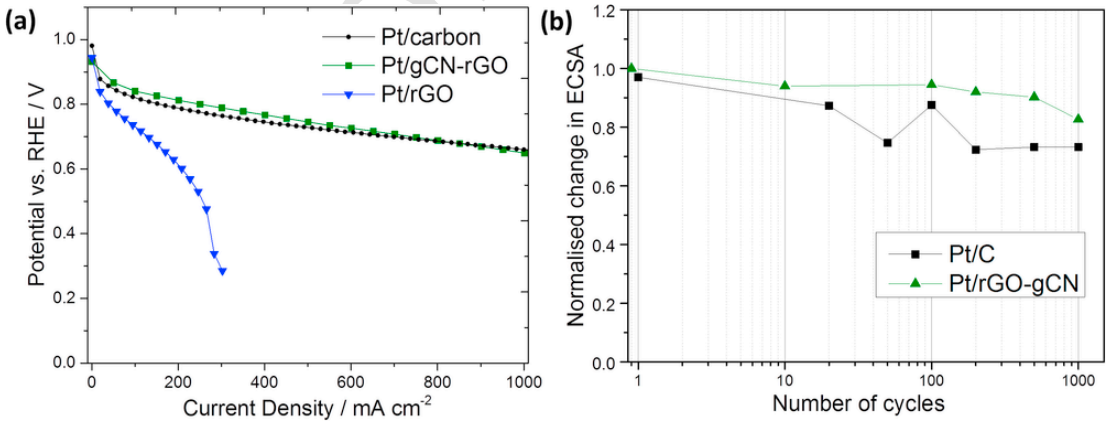

Fig. 6. (a) Fuel cell polarization curves of the Pt/C, Pt/gCNH-rGO and Pt/rGO as anode in H_2/O_2 cell at 80 °C. (d) Change in electrochemical surface area with respect to potential cycling (1.0–1.6 V) in 0.1 M $HClO_4$ at room temperature.

made from commercial melamine sponge [83] (Fig. 7). The resultant microporous structure exhibited a 3D interconnected network composed of 2D gCNH nanosheets with hierarchical pores ranging from 30–170 nm. The BET surface area was however low (40 $m^2 g^{-1}$). Other 3D frameworks incorporating gCNH, rGO or carbon nanotubes have been obtained *via* hydrothermal synthesis, followed by freeze-drying/supercritical drying [84,85], or by chemical crosslinking approaches [86]. Generally, in these methods, exfoliated gCNH nanosheets are homogeneously distributed in solution by mixing with GO and a 3D network is formed during a hydrothermal process, due to the partial removal of oxygen-containing groups from GO and restoration of van der Waals forces [85–88]. The dispersed gCNH nanosheets adhere onto the rGO surfaces and are thus incorporated in the 3D porous network [85,88]. One such 3D hybrid monolith produced by Huang et al. showed a BET surface area of up to 376 $m^2 g^{-1}$, with a hierarchical pore distribution ranging from sub-micrometer to several micrometers, along with a homogeneous dispersion of ultrafine Pt NPs (Fig. 8) [84]. This interconnected and porous catalyst system showed an excellent EC activity, high tolerance to poisoning, and reliable stability when used as anode ECs for DMFCs (Fig. 8d).

Recently we have also developed a 3D hybrid material, based upon a highly crystalline PTI rather than an amorphous gCNH [89]. Pt was deposited onto this 3D material *via* ethylene glycol reduction, yielding NPs with ~5 nm average size (Fig. 9). Preliminary tests using a rotating disk electrode showed that the Pt/PTI-rGO hybrid construct exhibited enhanced ORR activity, with at least ten-fold higher current density than Pt on pristine PTI at 0.90 V (Fig. 10). The material also displayed higher current density than Pt on rGO at 0.90 V, indicating that the combination of PTI and rGO improved the overall performance. Although the current density was lower than that of commercial Pt/C, these initial results are encouraging, considering the high durability of PTI. Further exploration of routes to enhance the interaction between gCNs and the conducting scaffold, the development of novel exfoliation pathways for gCNH and the improvement of methods to increase overall surface area and therefore access to N-containing catalytic sites, will significantly benefit applications for fuel cells.

4.3. Other gCN/C hybrid electrocatalysts and catalyst supports

Non-noble metal catalysts such as Fe and Co, supported on gCNH mixed/hybrids, have also been considered as alternative catalysts for the ORR and HOR [90–93]. Liu et al. reported excellent ORR electrocatalytic activity, comparable to commercial Pt/C with enhanced durability and methanol tolerance, for a Co-doped gCNH/graphene based catalyst under alkaline conditions [91]. They attributed this to the formation of Co-N moieties, which acted as active sites and promoted rapid charge transfer at the Co-gCNH/graphene interfaces. They further modified the catalyst and developed a novel core-shell structure with CoO as the core and Co-doped gCNH/graphene as the shell. The resulting hybrid displayed similar ORR catalytic activity, but with an improved stability due to the 'self-healing' ability of the oxide core that functioned as a source of cobalt, slowly releasing metal atoms or ions to heal the damaged active surface sites [92].

The use of composite materials involving gCNH materials doped with, for example, P and S as EC supports represents another field of investigation. For example, although its overall performance was still below that of commercial Pt/C, P-doped gCNH grown on flexible carbon fibre paper (CFP) has been shown to exhibit enhanced ORR activity compared to its phosphorous-free counterpart, and comparable to Pt supported on CFP [94]. 2D nanohybrid structures based on graphene quantum dots decorated onto sulphur-doped gCNH have also been developed. This unique S-gCN@GQD hybrid material has shown enhanced ORR catalytic activity, which was comparable to those of well-developed graphene and GQD based catalysts [95]. Such heteroatom-doped gCN hybrid materials are still far from commercial application, however they do present an interesting path for constructing new types of gCNH-based materials for energy conversion applications.

5. Integrated catalysts containing carbon nitride components

Di Noto et al. have defined "carbon nitride-based EC" (CN-based EC) supports as being composed of a carbon-based matrix into which nitrogen atoms have been embedded through synthesis reactions [45]. This family therefore includes all of the N-doped carbons, which have been extensively reviewed elsewhere [36] and that form structures ranging from N-doped mesoporous carbon [96] to N-doped car-

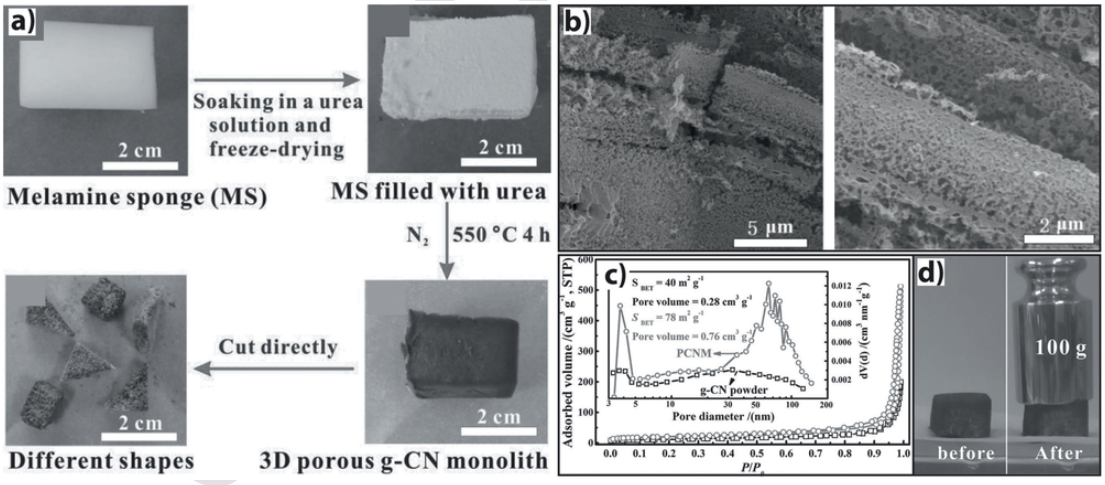

Fig. 7. 3D gCN structures (a) Schematic illustration of the preparation of a 3D porous gCN. (b) SEM and TEM images of porous g-C_3N_4 monolith. (c) N_2 sorption isotherms of the monolith. (d) Photographs of monolith showing that it could support a 100 g weight. Reprinted with permission from [83]. Copyright John Wiley and Sons.

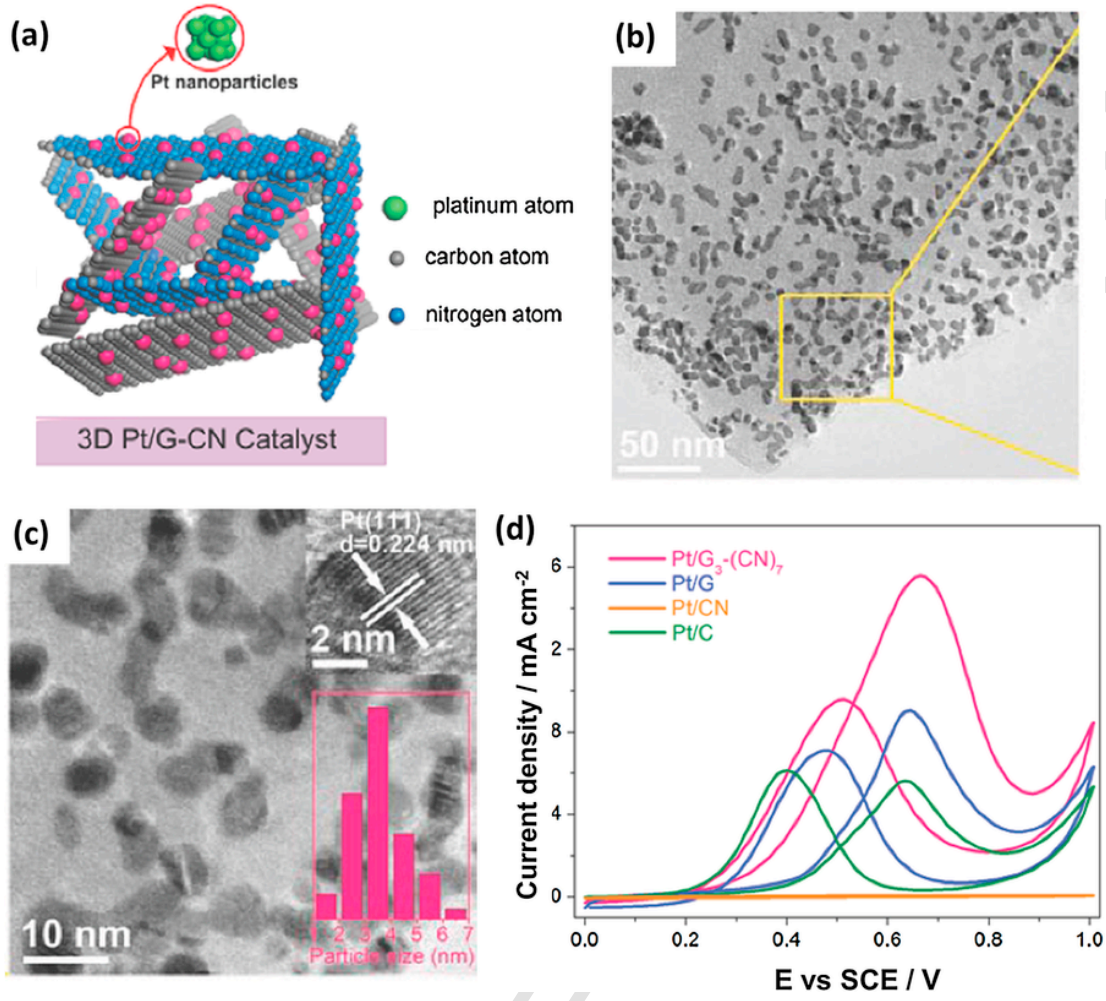

Fig. 8. 3D hybrid gCN structures. (a) Schematic illustration of 3D porous rGO-carbon nitride (CN) architectures prepared by hydrothermal reaction, Pt NPs are on the surfaces of both graphene and g-C_3N_4 nanosheets. (b, c) TEM morphological and structural analysis of a Pt on graphene-CN hybrid (3:7 ratio, Pt/G_3-$(CN)_7$), Insets in c: HRTEM image and Pt NP size distribution. (d) Cyclic voltammograms of the Pt/G-CN architecture (Pt/G_3-$(CN)_7$), Pt/G, Pt/CN and Pt/C in 1 M H_2SO_4 and 2 M methanol solution at a scan rate of 20 mV s^{-1}, reflecting the highest electrocatalytic activity of Pt/G_3-$(CN)_7$. Reprinted with permission from [84]. Copyright John Wiley and Sons.

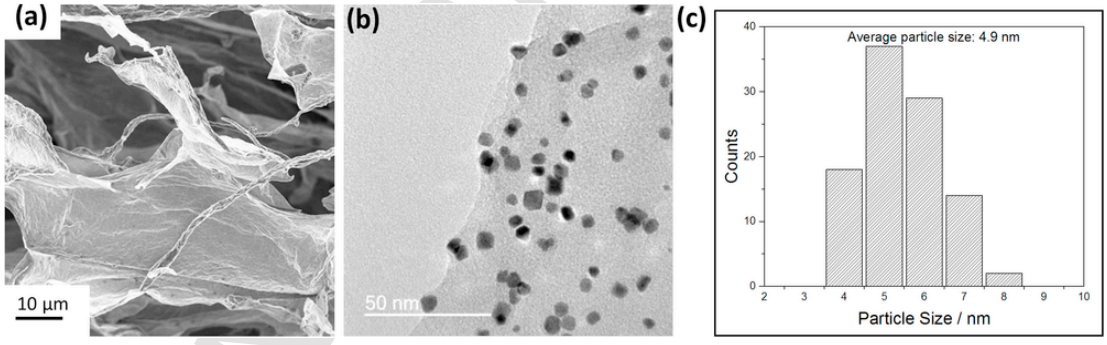

Fig. 9. Structure of PTI-rGO 3D hybrid aerogel catalyst support (a) SEM image of PTI-rGO 3D hybrid aerogel (b) TEM image of Pt dispersion on PTI-rGO hybrid aerogel. (c) Average particle size and size distribution of Pt nanoparticles.

bon nanotubes [43]. These materials generally have N contents <5 at% and they typically exhibit significantly different catalytic behavior to the gCN materials discussed above. CN-based ECs are often prepared by a one-pot synthesis, whereby solvated metal complexes and precursor molecules with high nitrogen content (either as one or multiple species) are adsorbed onto a carbon or carbonaceous precursor and the resultant composite material is pyrolyzed. The pyrolysis step acts to form the metal NPs and incorporate nitrogen into the carbon matrix [46,47]. In its simplest form this methodology has produced effective bulk electrocatalysts [46], but these materials have poorly defined structures and intrinsic irreproducibility, which has a

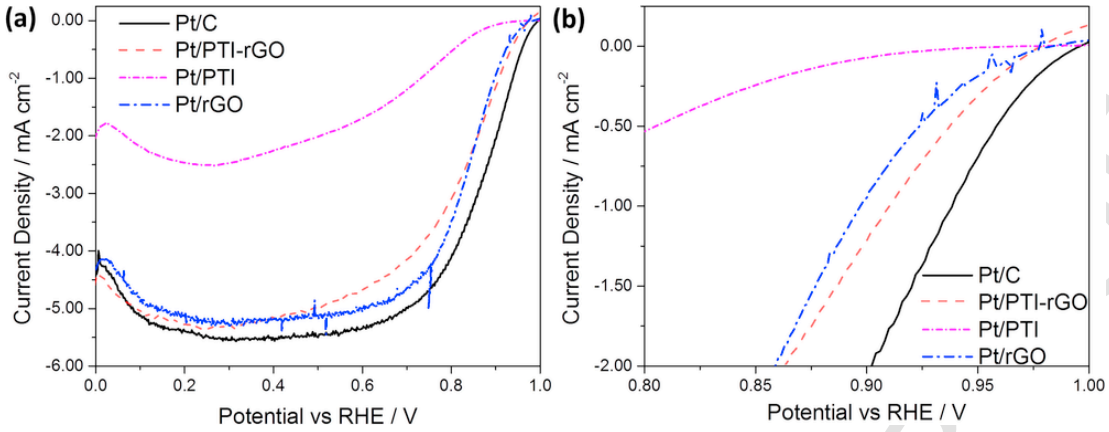

Fig. 10. Electrochemical testing of PTI and 3D PTI-rGO hybrid catalyst supports (a) ORR polarization curves of Pt supported on PTI, and rGO, and PTI-rGO hybrid, in comparison to commercial Pt/C (Alfa Aesar), at 1600 rpm in 0.1 M $HClO_4$. (b) Detail highlighting the ORR overpotential region.

significant impact on their overall efficacy and lifetime performance [45].

More recently, a new class of CN-based ECs has emerged in which there is a much more ordered and highly localized concentration of N atoms. This has been achieved by devising strategies to intelligently incorporate catalyst precursors within carbonaceous matrices [97–99]. Through the development of 3D-crosslinked inorganic-organic networks, Di Noto et al. were able to coordinate metal ions with macromolecular N-containing ligands, which, through the use of a two-step 'soft' pyrolysis technique, was than graphitized to form a foam-like conductive carbon matrix in which NPs were held in stabilizing 'N coordination nests' [45,97,98]. This method has been refined further through the introduction of a core-shell approach [100,101], whereby the metal and its surrounding N-containing matrix are constructed onto a conductive core. Through the use of these methods it was shown that the standard Pt NPs could be replaced with Pd in ORR ECs [102,103] or a bimetallic system [104], while still achieving a reduction in ORR overpotential *vs* Pt/C [105]. High Pt loading core-shell structures have also been described by Wu et al. [99]. These ECs showed improved activity for methanol oxidation over Pt/C due to higher Pt utilization and more rapid charge transfer, although here the Pt was deposited after the N-containing shell was constructed.

6. Carbon nitrides as catalyst supports for PEM water electrolyzers (PEMWEs)

PEMWEs are a promising technology for producing hydrogen from renewable, intermittent energy sources such as wind and photovoltaics [1,106,107]. PEMWEs have many advantages over the traditional alkaline electrolyzer systems, for example, they are capable of achieving current densities over 2 A cm^{-2}, reducing both operational and other costs of electrolysis [108]. In addition, PEMWE technologies provide very high purity hydrogen, giving the opportunity to obtain compressed gases directly from an installation. Furthermore, PWMEWs are ecologically clean, safer than other alternatives [109] and have a low gas crossover rate, allowing them to work over a wide range of power inputs [110]. However, current state-of-the-art PEMWEs also face significant challenges, mainly the need for relatively high loadings of precious metal ECs on both anode and cathode due to the corrosive acidic regime provided by the proton exchange membrane. These ECs must not only resist the corrosive low pH conditions (pH ~2), but must also sustain high applied overpotentials (~2 V), especially at high current densities [110].

Only a few materials, generally Pt group metals and their compounds, will perform effectively in operational PEMWE environments. Amongst those typically considered, the highest catalytic activity for the oxygen evolution reaction (OER) is exhibited by RuO_2. Unfortunately, this material corrodes at an appreciable rate with oxygen evolution [111] and hence must be stabilized by introduction of iridium or other elements. IrO_2 can be used as an alternative EC [112,113]. As with fuel cells, the high costs and low abundance of the catalytically active metals, has driven research into reducing their loading by dispersing them on low-cost supports that remain stable under operating conditions. Most approaches to-date have focused on supporting IrO_2 on materials such as TiO_2 [114], β-SiC [115], SnO_2 [116], Ta_2O_5 [117], Nb_2O_5 [118] and Sb_2O_5 [119]. Because gCN and gCNH materials have been attracting attention as fuel cell catalyst supports with potentially superior properties, it is of interest to study their performance in a PEMWE environment.

Jorge Sobrido et al. presented preliminary data for a bench scale, gCN-based, PEMWE operating at 50 °C and atmospheric pressure [120]. The results demonstrated that use of gCNH as a catalyst support at the anode improves the OER charge transfer kinetics and therefore the electrocatalytic activity (Fig. 11). Polarization measurements in this study showed high operating potentials for the gCNH supported EC, relative to unsupported IrO_2. However, the impedance data indicated that the gCNH supported IrO_2 has significantly smaller charge transfer resistance than the unsupported IrO_2 at higher current density, with the most significant loss associated with higher Ohmic resistance. This implies that there may be an avenue to optimize a gCNH-based electrode with reduced catalyst loading, although steps will need to be taken to improve the electronic conductivity of the catalyst.

7. Conclusion and outlook

Given the clear advantages associated with the incorporation of nitrogen into EC supports, there is great promise for future catalyst supports based on gCN materials. gCN supports have the potential to better anchor Pt and other metal NPs, improve the catalyst dispersion and durability, reduce the catalyst loading, and lead to improved catalyst performance. The results reviewed above demonstrate the progress already made with this this unique family of materials for EC development for fuel cell and electrolyzer applications. Now it will be necessary to cultivate a deeper understanding of the catalyst/support interactions and the role of the gCN or gCNH phases in determining the OER and ORR reaction kinetics. It is also essential to

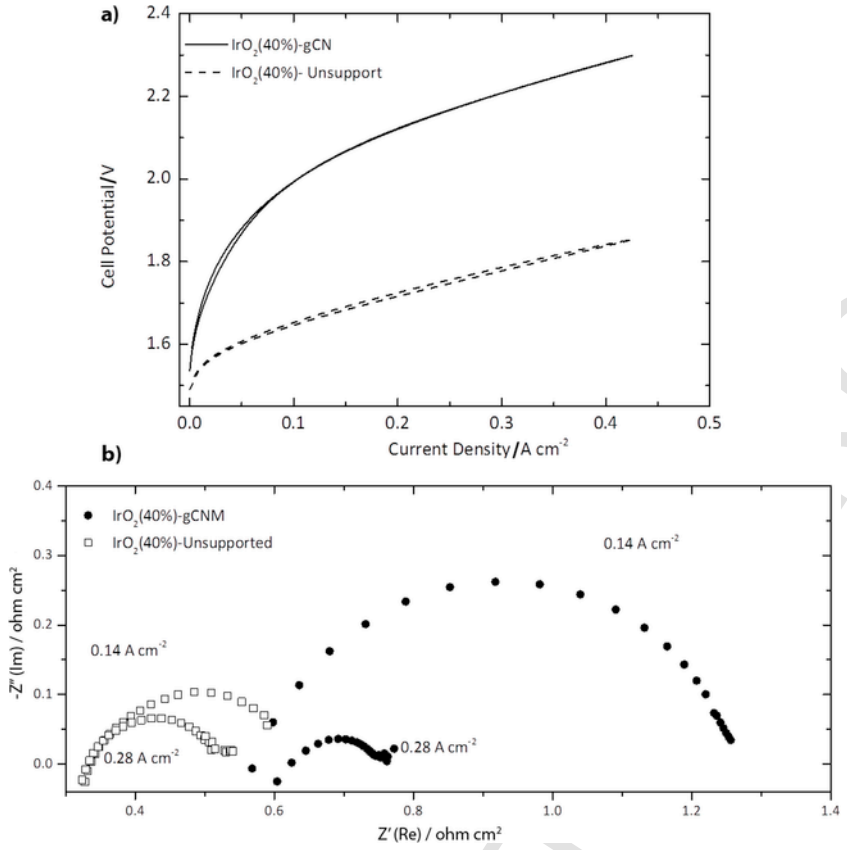

Fig. 11. Electrochemical data for unsupported IrO_2 (40%) and gCN supported IrO_2 (40%) as anode catalysts (both with 1.6 mg cm^{-2} metal loading) for a PEMWE. (a) Cell potential (V) *vs* current density measurements and (b) Nyquist plots of imaginary *vs* real parts of the complex impedance function (Z) for PEMWE tested with IrO_2 nanoparticles supported on gCN (IrO_2(40%)-gCNH) and pure IrO_2 nanoparticles (IrO_2(40%)-Unsupported) both of which were applied onto a Nafion membrane and used as anode electrocatalysts operating at 80 °C, ambient pressure.

optimize the gCN structure and chemistry, including the $C_xN_yH_z$ stoichiometry, and work on the incorporation of these materials in hybrid electrocatalysts and catalyst support combinations with high intrinsic catalytic activity, surface area and electrical conductivity. The continued development of new technological inks and 3D porous networks based on gCN materials is, likewise, an area for future development, as is the preparation of new families of integrated NP catalysts, where the active metal sites and protective N-rich regions are incorporated along with conductive graphene. As these new materials are investigated and efficient catalyst-support combinations identified and tested, it will be critically important to advance efficient, low-cost and scalable processes for their synthesis and commercial production, especially *via* drop-in technologies that can enter the marketplace rapidly.

Acknowledgements

This project has received funding from the European Union's Graphene Flagship under Horizon 2020 research and innovation programme grant agreement No. 696656 – GrapheneCore1 and from the EPSRCEP/L017091/1. C.M. acknowledges the award of a Royal Society University Research Fellowship by the UK Royal Society.

References

[1] European Commission, Hydrogen energy and fuel cells – a vision for our future, European Commission, Brussels, 2003.

[2] J. Spendelow, J. Marcinkoski, DOE fuel cell technologies office record 14012: Fuel cell system cost – 2013, Fuel Cell Technologies Office, 2013.

[3] U.S DRIVE Partnership, Fuel cell technical team roadmap, 2013.

[4] R. Jervis, D.J.L. Brett, Alkaline anion exchange membrane fuel cells, Materials for Low-Temperature Fuel Cells, Wiley-VCH Verlag GmbH & Co. KGaA, 20143–32.

[5] S. Mukerjee, Particle size and structural effects in platinum electrocatalysis, J. Appl. Electrochem. 20 (1990) 537–548.

[6] M. Shao, A. Peles, K. Shoemaker, Electrocatalysis on platinum nanoparticles: Particle size effect on oxygen reduction reaction activity, Nano Lett. 11 (2011) 3714–3719.

[7] G.A. Tritsaris, J. Greeley, J. Rossmeisl, J.K. Nørskov, Atomic-scale modeling of particle size effects for the oxygen reduction reaction on Pt, Catal. Lett. 141 (2011) 909–913.

[8] N.P. Brandon, D.J. Brett, Engineering porous materials for fuel cell applications, Phil. Trans. R. Soc. A: Mathematical, Physical and Engineering Sciences 364 (2006) 147–159.

[9] V.S. Bagotzky, A.M. Skundin, Electrocatalysts on supports—I. Electrochemical and adsorptive properties of platinum microdeposits on inert supports, Electrochim. Acta 29 (1984) 757–765.

[10] M.C. Román-Martínez, D. Cazorla-Amorós, A. Linares-Solano, C. Salinas-Martí'nez De Lecea, H. Yamashita, M. Anpo, Metal-support interaction in Pt/C catalysts. Influence of the support surface chemistry and the metal precursor, Carbon 33 (1995) 3–13.

[11] S.C. Hall, V. Subramanian, G. Teeter, B. Rambabu, Influence of metal–support interaction in Pt/C on CO and methanol oxidation reactions, Solid State Ionics 175 (2004) 809–813.

[12] R. Borup, J. Meyers, B. Pivovar, Y.S. Kim, R. Mukundan, N. Garland, D. Myers, M. Wilson, F. Garzon, D. Wood, P. Zelenay, K. More, K. Stroh, T. Zawodzinski, J. Boncella, J.E. McGrath, M. Inaba, K. Miyatake, M. Hori, K. Ota, Z. Ogumi, S. Miyata, A. Nishikata, Z. Siroma, Y. Uchimoto, K. Yasuda, K.-i. Kimijima, N. Iwashita, Scientific aspects of polymer electrolyte fuel cell durability and degradation, Chem. Rev. 107 (2007) 3904–3951.

[13] Y. Shao, G. Yin, Z. Wang, Y. Gao, Proton exchange membrane fuel cell from low temperature to high temperature: Material challenges, J. Power Sources 167 (2007) 235–242.
[14] P.T. Yu, W. Gu, J. Zhang, R. Makharia, F.T. Wagner, H.A. Gasteiger, Carbon-support requirements for highly durable fuel cell operation, in: F.N. Büchi, M. Inaba, T.J. Schmidt (Eds.), Polymer Electrolyte Fuel Cell Durability, Springer New York, New York, NY, 2009, pp. 29–53.
[15] A. Taniguchi, T. Akita, K. Yasuda, Y. Miyazaki, Analysis of electrocatalyst degradation in PEMFC caused by cell reversal during fuel starvation, J. Power Sources 130 (2004) 42–49.
[16] P.J. Ferreira, G.J. la O', Y. Shao-Horn, D. Morgan, R. Makharia, S. Kocha, H.A. Gasteiger, Instability of Pt/C electrocatalysts in proton exchange membrane fuel cells: A mechanistic investigation, J. Electrochem. Soc. 152 (2005) A2256–A2271.
[17] J.C. Meier, C. Galeano, I. Katsounaros, A.A. Topalov, A. Kostka, F. Schüth, K.J.J. Mayrhofer, Degradation mechanisms of Pt/C fuel cell catalysts under simulated start-stop conditions, ACS Catal. 2 (2012) 832–843.
[18] L.M. Roen, C.H. Paik, T.D. Jarvi, Electrocatalytic corrosion of carbon support in PEMFC cathodes, Electrochem. Solid-State Lett. 7 (2004) A19–A22.
[19] J. Willsau, J. Heitbaum, The influence of Pt-activation on the corrosion of carbon in gas diffusion electrodes—A DEMS study, J. Electroanal. Chem. Interfacial Electrochem. 161 (1984) 93–101.
[20] Z. Siroma, K. Ishii, K. Yasuda, Y. Miyazaki, M. Inaba, A. Tasaka, Imaging of highly oriented pyrolytic graphite corrosion accelerated by Pt particles, Electrochem. Commun. 7 (2005) 1153–1156.
[21] D.A. Stevens, J.R. Dahn, Thermal degradation of the support in carbon-supported platinum electrocatalysts for PEM fuel cells, Carbon 43 (2005) 179–188.
[22] E. Antolini, Carbon supports for low-temperature fuel cell catalysts, Appl. Catal. B 88 (2009) 1–24.
[23] E. Antolini, Graphene as a new carbon support for low-temperature fuel cell catalysts, Appl. Catal. B 123–124 (2012) 52–68.
[24] Y. Shao, J. Liu, Y. Wang, Y. Lin, Novel catalyst support materials for PEM fuel cells: current status and future prospects, J. Mater. Chem. 19 (2009) 46–59.
[25] S. Sharma, B.G. Pollet, Support materials for PEMFC and DMFC electrocatalysts—A review, J. Power Sources 208 (2012) 96–119.
[26] R.B. Kaner, J. Kouvetakis, C.E. Warble, M.L. Sattler, N. Bartlett, Boron-carbon-nitrogen materials of graphite-like structure, Mater. Res. Bull. 22 (1987) 399–404.
[27] O. Stephan, P.M. Ajayan, C. Colliex, P. Redlich, J.M. Lambert, P. Bernier, P. Lefin, Doping graphitic and carbon nanotube structures with boron and nitrogen, Science 266 (1994) 1683–1685.
[28] W. Cermignani, T.E. Paulson, C. Onneby, C.G. Pantano, Oxidation protection of carbon composites synthesis and characterization of boron-doped carbons, Carbon 33 (1995) 367–374.
[29] S. Wang, T. Cochell, A. Manthiram, Boron-doped carbon nanotube-supported Pt nanoparticles with improved CO tolerance for methanol electro-oxidation, PCCP 14 (2012) 13910–13913.
[30] S. Yang, L. Zhi, K. Tang, X. Feng, J. Maier, K. Müllen, Efficient synthesis of heteroatom (N or S)-doped graphene based on ultrathin graphene oxide-porous silica sheets for oxygen reduction reactions, Adv. Funct. Mater. 22 (2012) 3634–3640.
[31] Z. Yang, Z. Yao, G. Li, G. Fang, H. Nie, Z. Liu, X. Zhou, X. Chen, S. Huang, Sulfur-doped graphene as an efficient metal-free cathode catalyst for oxygen reduction, ACS Nano 6 (2012) 205–211.
[32] Y.J. Lee, L.R. Radovic, Oxidation inhibition effects of phosphorus and boron in different carbon fabrics, Carbon 41 (2003) 1987–1997.
[33] Z.W. Liu, F. Peng, H.J. Wang, H. Yu, W.X. Zheng, J. Yang, Phosphorus-doped graphite layers with high electrocatalytic activity for the O2 reduction in an alkaline medium, Angew. Chem. Int. Ed. 50 (2011) 3257–3261.
[34] Z. Liu, F. Peng, H. Wang, H. Yu, W. Zheng, X. Wei, Preparation of phosphorus-doped carbon nanospheres and their electrocatalytic performance for O2 reduction, J. Nat. Gas Chem. 21 (2012) 257–264.
[35] S. Pylypenko, A. Borisevich, K.L. More, A.R. Corpuz, T. Holme, A.A. Dameron, T.S. Olson, H.N. Dinh, T. Gennett, R. O'Hayre, Nitrogen: unraveling the secret to stable carbon-supported Pt-alloy electrocatalysts, Energy Environ. Sci. 6 (2013) 2957–2964.
[36] Y. Zhou, K. Neyerlin, T.S. Olson, S. Pylypenko, J. Bult, H.N. Dinh, T. Gennett, Z. Shao, R. O'Hayre, Enhancement of Pt and Pt-alloy fuel cell catalyst activity and durability via nitrogen-modified carbon supports, Energy Environ. Sci. 3 (2010) 1437–1446.
[37] S. Ye, A.K. Vijh, L.H. Dao, A new fuel cell electrocatalyst based on carbonized polyacrylonitrile foam: The nature of platinum-support interactions, J. Electrochem. Soc. 144 (1997) 90–95.
[38] N. Mansor, A.B. Jorge, F. Corà, C. Gibbs, R. Jervis, P.F. McMillan, X. Wang, D.J.L. Brett, Graphitic carbon nitride supported catalysts for polymer electrolyte fuel cells, J. Phys. Chem. C 118 (2014) 6831–6838.
[39] N. Mansor, A. Belen Jorge, F. Corà, C. Gibbs, R. Jervis, P.F. McMillan, X. Wang, D.J.L. Brett, Development of graphitic-carbon nitride materials as catalyst supports for polymer electrolyte fuel cells, ECS Trans. 58 (2013) 1767–1778.
[40] M. Kim, S. Hwang, J.-S. Yu, Novel ordered nanoporous graphitic C3N4 as a support for Pt-Ru anode catalyst in direct methanol fuel cell, J. Mater. Chem. 17 (2007) 1656–1659.
[41] E. Kroke, M. Schwarz, Novel group 14 nitrides, Coord. Chem. Rev. 248 (2004) 493–532.
[42] T.S. Miller, A. Belen Jorge, T.M. Suter, A. Sella, F. Corà, V. Brazdova, C. Howard, P.F. McMillan, Graphitic to polymeric carbon nitride materials: Characterisation to explain their physical properties, (in preparation).
[43] H.Y. Du, C.H. Wang, H.C. Hsu, S.T. Chang, U.S. Chen, S.C. Yen, L.C. Chen, H.C. Shih, K.H. Chen, Controlled platinum nanoparticles uniformly dispersed on nitrogen-doped carbon nanotubes for methanol oxidation, Diamond Relat. Mater. 17 (2008) 535–541.
[44] J. Shui, M. Wang, F. Du, L. Dai, N-doped carbon nanomaterials are durable catalysts for oxygen reduction reaction in acidic fuel cells, Sci. Adv 1 (2015) E1400129.
[45] V. Di Noto, E. Negro, K. Vezzù, F. Bertasi, G. Nawn, Origins, developments, and perspectives of carbon nitride-based electrocatalysts for application in low-temperature FCs, Electrochem. Soc. Interface 24 (2015) 59–64.
[46] S. Gupta, D. Tryk, I. Bae, W. Aldred, E. Yeager, Heat-treated polyacrylonitrile-based catalysts for oxygen electroreduction, J. Appl. Electrochem. 19 (1989) 19–27.
[47] J.A.R. van Veen, J.F. van Baar, K.J. Kroese, Effect of heat treatment on the performance of carbon-supported transition-metal chelates in the electrochemical reduction of oxygen, J. Chem. Soc. Faraday Trans. 1 77 (1981) 2827–2843.
[48] H. Wang, T. Maiyalagan, X. Wang, Review on recent progress in nitrogen-doped graphene: Synthesis, characterization, and its potential applications, ACS Catal. 2 (2012) 781–794.
[49] R. Czerw, M. Terrones, J.C. Charlier, X. Blase, B. Foley, R. Kamalakaran, N. Grobert, H. Terrones, D. Tekleab, P.M. Ajayan, W. Blau, M. Rühle, D.L. Carroll, Identification of electron donor states in N-doped carbon nanotubes, Nano Lett. 1 (2001) 457–460.
[50] K.N. Wood, R. O'Hayre, S. Pylypenko, Recent progress on nitrogen/carbon structures designed for use in energy and sustainability applications, Energy Environ. Sci. 7 (2014) 1212–1249.
[51] A. Schwarzer, T. Saplinova, E. Kroke, Tri-s-triazines (s-heptazines)—From a mystery molecule to industrially relevant carbon nitride materials, Coord. Chem. Rev. 257 (2013) 2032–2062.
[52] B.V. Lotsch, M. Döblinger, J. Sehnert, L. Seyfarth, J. Senker, O. Oeckler, W. Schnick, Unmasking melon by a complementary approach employing electron diffraction, solid-state NMR spectroscopy, and theoretical calculations—structural characterization of a carbon nitride polymer, Chem. Eur. J. 13 (2007) 4969–4980.
[53] J. Kouvetakis, M. Todd, B. Wilkens, A. Bandari, N. Cave, Novel synthetic routes to carbon-nitrogen thin films, Chem. Mater. 6 (1994) 811–814.
[54] M. Todd, J. Kouvetakis, T.L. Groy, D. Chandrasekhar, D.J. Smith, P.W. Deal, Novel synthetic routes to carbon nitride, Chem. Mater. 7 (1995) 1422–1426.
[55] G. Algara-Siller, N. Severin, S.Y. Chong, T. Björkman, R.G. Palgrave, A. Laybourn, M. Antonietti, Y.Z. Khimyak, A.V. Krasheninnikov, J.P. Rabe, U. Kaiser, A.I. Cooper, A. Thomas, M.J. Bojdys, Triazine-based graphitic carbon nitride: A two-dimensional semiconductor, Angew. Chem. Int. Ed. 53 (2014) 7450–7455.
[56] M.J. Bojdys, J.-O. Müller, M. Antonietti, A. Thomas, Ionothermal synthesis of crystalline condensed, graphitic carbon nitride, Chem. Eur. J. 14 (2008) 8177–8182.
[57] E.J. McDermott, E. Wirnhier, W. Schnick, K.S. Virdi, C. Scheu, Y. Kauffmann, W.D. Kaplan, E.Z. Kurmaev, A. Moewes, Band gap tuning in poly(triazine imide), a nonmetallic photocatalyst, J. Phys. Chem. C 117 (2013) 8806–8812.
[58] E. Wirnhier, M. Döblinger, D. Gunzelmann, J. Senker, B.V. Lotsch, W. Schnick, Poly(triazine imide) with intercalation of lithium and chloride ions [(C3N3)2(NHxLi1-x)3·LiCl]: A crystalline 2D carbon nitride network, Chem. Eur. J. 17 (2011) 3213–3221.
[59] S.Y. Chong, J.T.A. Jones, Y.Z. Khimyak, A.I. Cooper, A. Thomas, M. Antonietti, M.J. Bojdys, Tuning of gallery heights in a crystalline 2D carbon nitride network, J. Mater. Chem. A 1 (2013) 1102–1107.
[60] Z. Zhang, K. Leinenweber, M. Bauer, L.A.J. Garvie, P.F. McMillan, G.H. Wolf, High-pressure bulk synthesis of crystalline C6N9H3·HCl: A novel C3N4 graphitic derivative, J. Am. Chem. Soc. 123 (2001) 7788–7796.
[61] X. Wang, K. Maeda, A. Thomas, K. Takanabe, G. Xin, J.M. Carlsson, K. Domen, M. Antonietti, A metal-free polymeric photocatalyst for hydrogen production from water under visible light, Nat Mater 8 (2009) 76–80.
[62] Y. Wang, Y. Di, M. Antonietti, H. Li, X. Chen, X. Wang, Excellent visible-light photocatalysis of fluorinated polymeric carbon nitride solids, Chem. Mater. 22 (2010) 5119–5121.
[63] A. Thomas, A. Fischer, F. Goettmann, M. Antonietti, J.O. Muller, R. Schlogl, J.M. Carlsson, Graphitic carbon nitride materials: variation of structure and morphology and their use as metal-free catalysts, J. Mater. Chem. 18 (2008) 4893–4908.

[64] Y. Wang, X. Wang, M. Antonietti, Polymeric graphitic carbon nitride as a heterogeneous organocatalyst: From photochemistry to multipurpose catalysis to sustainable chemistry, Angew. Chem. Int. Ed. 51 (2012) 68–89.
[65] T.S. Miller, A.B. Jorge, A. Sella, F. Corà, P.R. Shearing, D.J.L. Brett, P.F. McMillan, The use of graphitic carbon nitride based composite anodes for lithium-ion battery applications, Electroanalysis 27 (2015) 2614–2619.
[66] G.M. Veith, L. Baggetto, L.A. Adamczyk, B. Guo, S.S. Brown, X.-G. Sun, A.A. Albert, J.R. Humble, C.E. Barnes, M.J. Bojdys, S. Dai, N.J. Dudney, Electrochemical and solid-state lithiation of graphitic C3N4, Chem. Mater. 25 (2013) 503–508.
[67] S.M. Lyth, Y. Nabae, S. Moriya, S. Kuroki, M. Kakimoto, J. Ozaki, S. Miyata, Carbon nitride as a nonprecious catalyst for electrochemical oxygen reduction, J. Phys. Chem. C 113 (2009) 20148–20151.
[68] Y. Wang, J. Zhang, X. Wang, M. Antonietti, H. Li, Boron- and Fluorine-Containing Mesoporous Carbon Nitride Polymers: Metal-Free Catalysts for Cyclohexane Oxidation, Angew. Chem. Int. Ed. 49 (2010) 3356–3359.
[69] Y. Zheng, Y. Jiao, J. Chen, J. Liu, J. Liang, A. Du, W. Zhang, Z. Zhu, S.C. Smith, M. Jaroniec, G.Q. Lu, S.Z. Qiao, Nanoporous graphitic-C3N4@carbon metal-free electrocatalysts for highly efficient oxygen reduction, J. Am. Chem. Soc. 133 (2011) 20116–20119.
[70] S. Yang, X. Feng, X. Wang, K. Müllen, Graphene-based carbon nitride nanosheets as efficient metal-free electrocatalysts for oxygen reduction reactions, Angew. Chem. Int. Ed. 50 (2011) 5339–5343.
[71] J. Liang, Y. Zheng, J. Chen, J. Liu, D. Hulicova-Jurcakova, M. Jaroniec, S.Z. Qiao, Facile oxygen reduction on a three-dimensionally ordered macroporous graphitic C3N4/carbon composite electrocatalyst, Angew. Chem. Int. Ed. 51 (2012) 3892–3896.
[72] C. Song, S. Kim, Preparation and electrochemical characterization of Pt-supported flake-like graphitic carbon nitride on reduced graphene oxide as fuel cell catalysts, J. Electrochem. Soc. 162 (2015) F1181–F1190.
[73] C.Z. Li, Z.B. Wang, X.L. Sui, L.M. Zhang, D.M. Gu, Ultrathin graphitic carbon nitride nanosheets and graphene composite material as high-performance PtRu catalyst support for methanol electro-oxidation, Carbon 93 (2015) 105–115.
[74] C. Hu, Q. Han, F. Zhao, Z. Yuan, N. Chen, L. Qu, Graphitic C3N4-Pt nanohybrids supported on a graphene network for highly efficient methanol oxidation, Science China Materials 58 (2015) 21–27.
[75] A. Du, S. Sanvito, Z. Li, D. Wang, Y. Jiao, T. Liao, Q. Sun, Y.H. Ng, Z. Zhu, R. Amal, S.C. Smith, Hybrid graphene and graphitic carbon nitride nanocomposite: Gap opening, electron-hole puddle, interfacial charge transfer, and enhanced visible light response, J. Am. Chem. Soc. 134 (2012) 4393–4397.
[76] K. Qiu, Z.X. Guo, Hierarchically porous graphene sheets and graphitic carbon nitride intercalated composites for enhanced oxygen reduction reaction, J. Mater. Chem. A 2 (2014) 3209–3215.
[77] Y. Sun, C. Li, Y. Xu, H. Bai, Z. Yao, G. Shi, Chemically converted graphene as substrate for immobilizing and enhancing the activity of a polymeric catalyst, Chem. Commun. 46 (2010) 4740–4742.
[78] W. Zhang, H. Huang, F. Li, K. Deng, X. Wang, Palladium nanoparticles supported on graphitic carbon nitride-modified reduced graphene oxide as highly efficient catalysts for formic acid and methanol electrooxidation, J. Mater. Chem. A 2 (2014) 19084–19094.
[79] Z. Li, R. Lin, Z. Liu, D. Li, H. Wang, Q. Li, Novel graphitic carbon nitride/graphite carbon/palladium nanocomposite as a high-performance electrocatalyst for the ethanol oxidation reaction, Electrochim. Acta 191 (2016) 606–615.
[80] N. Mansor, T.S. Miller, J. Jia, C. Mattevi, C. Gibbs, D. Hodgson, M. Shaffer, D.J.L. Brett, P.F. McMillan, Graphitic carbon nitride – graphene hybrid as a catalyst support for polymer electrolyte membrane fuel cells, (in preparation).
[81] Y. Garsany, I.L. Singer, K.E. Swider-Lyons, Impact of film drying procedures on RDE characterization of Pt/VC electrocatalysts, J. Electroanal. Chem. 662 (2011) 396–406.
[82] W. Sheng, H.A. Gasteiger, Y. Shao-Horn, Hydrogen oxidation and evolution reaction kinetics on platinum: Acid vs alkaline electrolytes, J. Electrochem. Soc. 157 (2010) B1529–B1536.
[83] Q. Liang, Z. Li, X. Yu, Z.H. Huang, F. Kang, Q.H. Yang, Macroscopic 3d porous graphitic carbon nitride monolith for enhanced photocatalytic hydrogen evolution, Adv. Mater. 27 (2015) 4634–4639.
[84] H. Huang, S. Yang, R. Vajtai, X. Wang, P.M. Ajayan, Pt-decorated 3D architectures built from graphene and graphitic carbon nitride nanosheets as efficient methanol oxidation catalysts, Adv. Mater. 26 (2014) 5160–5165.
[85] T.Y. Ma, S. Dai, M. Jaroniec, S.Z. Qiao, Graphitic carbon nitride nanosheet-carbon nanotube three-dimensional porous composites as high-performance oxygen evolution electrocatalysts, Angew. Chem. Int. Ed. 53 (2014) 7281–7285.
[86] M. De Marco, F. Markoulidis, R. Menzel, S.M. Bawaked, M. Mokhtar, S.A. Al-Thabaiti, S.N. Basahel, M.S.P. Shaffer, Cross-linked single-walled carbon nanotube aerogel electrodes via reductive coupling chemistry, J. Mater. Chem. A 4 (2016) 5385–5389.
[87] C. Li, G. Shi, Functional gels based on chemically modified graphenes, Adv. Mater. 26 (2014) 3992–4012.
[88] W.J. Ong, L.L. Tan, S.P. Chai, S.T. Yong, A.R. Mohamed, Surface charge modification via protonation of graphitic carbon nitride (g-C3N4) for electrostatic self-assembly construction of 2D/2D reduced graphene oxide (rGO)/g-C3N4 nanostructures toward enhanced photocatalytic reduction of carbon dioxide to methane, Nano Energy 13 (2015) 757–770.
[89] N. Mansor, J. Jia, T.S. Miller, C. Mattevi, C. Gibbs, D. Hodgson, M. Shaffer, D.J.L. Brett, P.F. McMillan, Poly(triazine imide) based composites as electrocatalyst support for fuel cells, (in preparation).
[90] M.K. Kundu, T. Bhowmik, S. Barman, Gold aerogel supported on graphitic carbon nitride: an efficient electrocatalyst for oxygen reduction reaction and hydrogen evolution reaction, J. Mater. Chem. A 3 (2015) 23120–23135.
[91] Q. Liu, J. Zhang, Graphene supported Co-g-C3N4 as a novel metal–macrocyclic electrocatalyst for the oxygen reduction reaction in fuel cells, Langmuir 29 (2013) 3821–3828.
[92] J. Jin, X. Fu, Q. Liu, J. Zhang, A highly active and stable electrocatalyst for the oxygen reduction reaction based on a graphene-supported g-C3N4@cobalt oxide core-shell hybrid in alkaline solution, J. Mater. Chem. A 1 (2013) 10538–10545.
[93] J.J. Feng, L.X. Chen, P. Song, X. Wu, A.J. Wang, J. Yuan, Bimetallic AuPd nanoclusters supported on graphitic carbon nitride: One-pot synthesis and enhanced electrocatalysis for oxygen reduction and hydrogen evolution, Int. J. Hydrogen Energy 41 (2016) 8839–8846.
[94] T.Y. Ma, J. Ran, S. Dai, M. Jaroniec, S.Z. Qiao, Phosphorus-doped graphitic carbon nitrides grown in situ on carbon-fiber paper: Flexible and reversible oxygen electrodes, Angew. Chem. Int. Ed. 54 (2015) 4646–4650.
[95] C. Xu, Q. Han, Y. Zhao, L. Wang, Y. Li, L. Qu, Sulfur-doped graphitic carbon nitride decorated with graphene quantum dots for an efficient metal-free electrocatalyst, J. Mater. Chem. A 3 (2015) 1841–1846.
[96] Z. Lei, L. An, L. Dang, M. Zhao, J. Shi, S. Bai, Y. Cao, Highly dispersed platinum supported on nitrogen-containing ordered mesoporous carbon for methanol electrochemical oxidation, Microporous Mesoporous Mater. 119 (2009) 30–38.
[97] V. Di Noto, E. Negro, R. Gliubizzi, S. Gross, C. Maccato, G. Pace, Pt and Ni carbon nitride electrocatalysts for the oxygen reduction reaction, J. Electrochem. Soc. 154 (2007) B745–B756.
[98] V. Di Noto, A novel polymer electrolyte based on oligo(ethylene glycol) 600, K2PdCl4, and K3Fe(CN)6, J. Mater. Res. 12 (1997) 3393–3403.
[99] G. Wu, D. Li, C. Dai, D. Wang, N. Li, Well-dispersed high-loading Pt nanoparticles supported by shell-core nanostructured carbon for methanol electrooxidation, Langmuir 24 (2008) 3566–3575.
[100] E. Negro, K. Vezzu, F. Bertasi, P. Schiavuta, L. Toniolo, S. Polizzi, V. Di Noto, Interplay between nitrogen concentration, structure, morphology, and electrochemical performance of PdCoNi core-shell carbon nitride electrocatalysts for the oxygen reduction reaction, Chemelectrochem 1 (2014) 1359–1369.
[101] V. Di Noto, E. Negro, Pt-Fe and Pt-Ni carbon nitride-based ‘core-shell' ORR electrocatalysts for polymer electrolyte membrane fuel cells, Fuel Cells 10 (2010) 234–244.
[102] V. Di Noto, E. Negro, Development of nano-electrocatalysts based on carbon nitride supports for the ORR processes in PEM fuel cells, Electrochim. Acta 55 (2010) 7564–7574.
[103] V. Di Noto, E. Negro, Synthesis, characterization and electrochemical performance of tri-metal Pt-free carbon nitride electrocatalysts for the oxygen reduction reaction, Electrochim. Acta 55 (2010) 1407–1418.
[104] V. Di Noto, E. Negro, A new Pt–Rh carbon nitride electrocatalyst for the oxygen reduction reaction in polymer electrolyte membrane fuel cells: Synthesis, characterization and single-cell performance, J. Power Sources 195 (2010) 638–648.
[105] V. Di Noto, E. Negro, G.A. Giffin, (Keynote lecture) multi-metal nano-electrocatalysts based on carbon nitride supports for the ORR and for in PEM fuel cells, ECS Trans. 40 (2012) 3–10.
[106] F. Barbir, PEM electrolysis for production of hydrogen from renewable energy sources, Sol. Energy 78 (2005) 661–669.
[107] D. Ipsakis, S. Voutetakis, P. Seferlis, F. Stergiopoulos, C. Elmasides, Power management strategies for a stand-alone power system using renewable energy sources and hydrogen storage, Int. J. Hydrogen Energy 34 (2009) 7081–7095.
[108] I. Dedigama, P. Angeli, N. van Dijk, J. Millichamp, D. Tsaoulidis, P.R. Shearing, D.J.L. Brett, Current density mapping and optical flow visualisation of a polymer electrolyte membrane water electrolyser, J. Power Sources 265 (2014) 97–103.
[109] R. Balaji, N. Senthil, S. Vasudevan, S. Ravichandran, S. Mohan, G. Sozhan, S. Madhu, J. Kennedy, S. Pushpavanam, M. Pushpavanam, Development and performance evaluation of Proton Exchange Membrane (PEM) based hydrogen generator for portable applications, Int. J. Hydrogen Energy 36 (2011) 1399–1403.
[110] M. Carmo, D.L. Fritz, J. Mergel, D. Stolten, A comprehensive review on PEM water electrolysis, Int. J. Hydrogen Energy 38 (2013) 4901–4934.
[111] C. Iwakura, K. Hirao, H. Tamura, Anodic evolution of oxygen on ruthenium in acidic solutions, Electrochim. Acta 22 (1977) 329–334.

[112] S. Song, H. Zhang, X. Ma, Z. Shao, R.T. Baker, B. Yi, Electrochemical investigation of electrocatalysts for the oxygen evolution reaction in PEM water electrolyzers, Int. J. Hydrogen Energy 33 (2008) 4955–4961.
[113] T.I. Valdez, K.J. Billings, J. Sakamoto, F. Mansfeld, S.R. Narayanan, Iridium and lead doped ruthenium oxide catalysts for oxygen evolution, ECS Trans. 25 (2009) 1371–1382.
[114] P. Mazúr, J. Polonský, M. Paidar, K. Bouzek, Non-conductive TiO2 as the anode catalyst support for PEM water electrolysis, Int. J. Hydrogen Energy 37 (2012) 12081–12088.
[115] J. Polonský, P. Mazúr, M. Paidar, K. Bouzek, Investigation of β-SiC as an anode catalyst support for PEM water electrolysis, J. Solid State Electrochem. 18 (2014) 2325–2332.
[116] C.P. De Pauli, S. Trasatti, Electrochemical surface characterization of IrO2 + SnO2 mixed oxide electrocatalysts, J. Electroanal. Chem. 396 (1995) 161–168.
[117] M. Morimitsu, R. Otogawa, M. Matsunaga, Effects of cathodizing on the morphology and composition of IrO2. Ta2O5/Ti anodes, Electrochim. Acta 46 (2000) 401–406.
[118] A.J. Terezo, J. Bisquert, E.C. Pereira, G. Garcia-Belmonte, Separation of transport, charge storage and reaction processes of porous electrocatalytic IrO2 and IrO2/Nb2O5 electrodes, J. Electroanal. Chem. 508 (2001) 59–69.
[119] G. Chen, X. Chen, P.L. Yue, Electrochemical behavior of novel Ti/IrOx-Sb2O5-SnO2 anodes, J. Phys. Chem. B 106 (2002) 4364–4369.
[120] A.B. Jorge Sobrido, I. Dedigama, N. Mansor, R. Jervis, T.S. Miller, F. Corà, P. Shearing, C. Gibbs, P.F. McMillan, D.J. Brett, Graphitic carbon nitride materials for energy applications, ECS Trans. 64 (2015) 13–30.